Linear Instability Analysis of Natural Convection in a Heated Vertical Porous Annulus

A. Khan, P. Chokshi, and P. Bera

Abstract The stability analysis of non-isothermal annular parallel flow through a highly permeable porous medium is studied. The flow is governed by the buoyancy force induced due to the different temperature conditions on the surface of inner and outer cylinders. A linear stability analysis subjected to normal mode analysis has been considered to investigate the influence of gap between cylinders (defined by the curvature parameter, C), Darcy number (Da, which is defined in terms of permeability of the porous medium) as well as Prandtl number (Pr) on the flow instability characteristics. The existence of the inflection point in the laminar base flow profile is checked. Depending on the value of controlling parameters (C, Pr, and Da), the least stable disturbance is found to be axisymmetric for smaller gap and non-axisymmetric for a larger gap between cylinders. The physical mechanism of the flow instability has been examined through kinetic energy analysis.

Keywords Natural convection · Porous media flow · Linear stability theory

1 Introduction

The natural convection in a vertically oriented porous slab/duct has been thoroughly explored due to its practical relevance appeared in electronic industry, thermal-hydraulics of nuclear reactors [1], chemical processing equipment [2], geothermal engineering [3] and building engineering [4]. Knowledge of the heat transfer characteristics and fluid flow mechanism for duct flow systems can guide in optimization of the thermal design and ensure a high degree of safety in the devices used in these applications. As a result, understanding the flow dynamics and heat transfer mechanism under different geometry is crucial before initializing the duct flow through

A. Khan (✉) · P. Chokshi
Department of Chemical Engineering, IIT Delhi, New Delhi 110016, India
e-mail: arshan.khan792@gmail.com

P. Bera
Department of Mathematics, IIT Roorkee, Roorkee 247667, India

K. M. Singh et al. (eds.), *Fluid Mechanics and Fluid Power, Volume 2*, Lecture Notes in Mechanical Engineering, https://doi.org/10.1007/978-981-99-5752-1_3

porous media in any appliance. The storage of nuclear wastes is another significant application of the flow through vertical porous slab, and it is essential to determine the insulating impact of the annular air gap surrounding a cylindrical nuclear waste canister implanted in a geologic repository. In such a situation, the temperature of the canister is critical because it is the primary factor that determines the life span of the metal containers. To determine if heat will be transferred through the air gap by conduction or convection, the stability of the parallel motion must be investigated.

Generally, the flow through porous medium can be show to depend on the Prandtl number (Pr), Grashof number (Gr), permeability of the porous medium and geometry of the porous enclosure. There are numerous studies that explore the influence of Pr and the media permeability on the instability characteristics of natural convection in a rectangular channel saturated with porous material, which are well documented in refs. [5, 6] and references therein. The annular flow is unlike the conventional channel flow in terms of heat transfer mechanism and the flow instability characteristic [7]. Based on the gap between circular coaxial cylinders, the study of the annular flow provides a more general overview of the duct flow (including channel flow as well as flow through a circular pipe with a thin rod its center) dynamics. Therefore, motivated by the strikingly different stability characteristics of the flow in annular configuration compared to the flow in channel and the use of annular set up in many industrial situations [8], an extension of the work of Khan and Bera [9] to the natural convection case is established in the present study. From the best of our knowledge, there are only two studies [10, 11] on the stability of a natural convection in a vertical annulus filled with porous media. These studies are restricted to the stationary base flow. They have only looked into the effect of radius ratio (or curvature parameter), ignoring the effects of the permeability of the porous medium and the type of fluid in terms of Prandtl number. In a tall vertical slot, if the flow is assumed to be parallel, the velocity profile persists a nonlinear shape, with the fluid moving downward near the cooler wall and upward near the warmer wall [12]. It has been observed for the purely viscous media flow through vertical annulus. In a parallel flow, the flow is said to be in the conduction regime since heat is only carried across the duct by conduction between the fluid layers. The conduction regime when Gr is small was also validated by the experimental data [13]. However, as Gr rises, the flow becomes unstable, first giving rise to multicellular secondary flow patterns and then, as Gr rises even higher, turbulence. It has also been studied into whether the natural convection conduction regime is stable [14]. The Pr effects on the flow instabilities of natural convection in annular geometry filled with isotropic porous material have never been studied. Therefore, a step has been taken in the present work to understand such instability characteristics. Here, we have focused on the Prandtl number, curvature parameter (characterized in terms of the gap between cylinders), and media permeability on the type of instability and have been shown that these parameters are also responsible for the resulting type of insatiability and heat transport in the annular domain.

2 Methodology

The problem under consideration is the natural convection in a vertically oriented annular passage filled with isotropic porous material. The annulus is delimited by homogeneous and isotropic porous layers. The inner wall of the annulus is kept at constant heat flux and the outer wall is insulated. The fluid's thermo-physical properties are considered to be constant except for the dependence of the buoyancy force term in the momentum equation on the fluid density, which is satisfied by the Boussinesq approximation. For the present theoretical investigation, we consider the Darcy-Brinkman model including the local time derivative based on the volume-averaged Navier–Stokes equations developed by Whitaker [15].

After scaling the dimensional variables, the non-dimensional space coordinates (n, ψ, z), dependent variables (u, v, w, θ, p) and time t are determined as follows:

$$(u, v, w) = \frac{(u^*, v^*, w^*)}{w_s^*}, z = \frac{z^*}{(r_o - r_i)}, \eta = \frac{(r^* - r_i)}{(r_o - r_i)},$$
$$\theta = \frac{(T_w - T^*)\nu}{k(r_o - r_i)^2}, p = \frac{p^*}{\rho_f w_s^{*2}}, t = \frac{t^* w_s^*}{(r_o - r_i)^2},$$

here w_s^* is defined as $g\beta k(r_o - r_i)^4/\nu^2$, which can be obtained by balancing the buoyancy force and viscous force in the vertical momentum equation. The non-dimensional governing equations for continuity, momentum and energy, after dropping asterisks, in cylindrical coordinate (n, ψ, z), are given as

$$\frac{\partial u}{\partial \eta} + \frac{u}{(\eta + C)} + \frac{1}{(\eta + C)}\frac{\partial v}{\partial \psi} + \frac{\partial w}{\partial z} = 0, \tag{1}$$

$$\frac{1}{\epsilon}\frac{\partial u}{\partial t} = -\frac{\partial p}{\partial \eta} + \frac{1}{Gr}\left[D^2 u - \frac{2}{(\eta + C)^2}\frac{\partial v}{\partial \psi} - \frac{u}{(\eta + C)^2}\right] - \frac{1}{Gr\,Da}u, \tag{2}$$

$$\frac{1}{\varepsilon}\frac{\partial v}{\partial t} = -\frac{1}{\eta + C}\frac{\partial p}{\partial \psi} + \frac{1}{Gr}\left[D^2 v + \frac{2}{(\eta + C)^2}\frac{\partial u}{\partial \psi} - \frac{v}{(\eta + C)^2}\right] - \frac{1}{Gr\,Da}v, \tag{3}$$

$$\frac{1}{\varepsilon}\frac{\partial w}{\partial t} = -\frac{\partial p}{\partial z} + \frac{1}{Gr}\left[D^2 w - \frac{1}{Da}w - \theta\right], \tag{4}$$

$$\sigma\frac{\partial \theta}{\partial t} + u\frac{\partial \theta}{\partial \eta} + \frac{v}{\eta + c}\frac{\partial \theta}{\partial \psi} + w\frac{\partial \theta}{\partial z} = \frac{1}{Gr\,Pr}\left[D^2\theta + \sigma\right], \tag{5}$$

where,

$$D^2 = \frac{\partial^2}{\partial \eta^2} + \frac{1}{\eta + C}\frac{\partial}{\partial \eta} + \frac{1}{(\eta + C)^2}\frac{\partial^2}{\partial \psi^2} + \frac{\partial^2}{\partial z^2}.$$

The used dimensionless parameters in the governing equations are the curvature parameter, $C = \frac{r_i}{r_o - r_i}$, porosity, ε, the Grashof number, $Gr = \frac{w_s(r_o - r_i)}{\nu}$, the Darcy number, $Da = \frac{K}{(r_o - r_i)^2}$, ratio of specific heat capacities, $\sigma = \frac{c_p}{c_v}$ and the Prandtl number, $Pr = \frac{\nu}{\alpha}$. Here $r_i, r_o, \nu, K, c_p, c_v, \alpha$ and ρ are the radius of inner cylinder, radius of outer cylinder, kinematic viscosity, permeability of the porous medium, specific heat capacity at constant pressure, specific heat capacity at constant volume, thermal diffusivity and the density of the fluid phase, respectively. To avoid too many parametric studies, we have fixed the heat capacity ratio at 1.

2.1 Basic Flow Equations

The basic flow, whose stability will be analyzed, is a steady, unidirectional and fully developed flow. Using these assumptions to Eqs. (2)-(6), the basic flow becomes independent of the axial and azimuthal coordinates and the simplified governing equations are

$$W'' + \frac{1}{\eta + C} W' - \frac{1}{Da} W - \Theta = Gr \frac{dP}{dz} \tag{6}$$

$$\Theta'' + \frac{1}{\eta + C} \Theta' = -1 \tag{7}$$

where W, P and Θ are the basic velocity, pressure and temperature, respectively. The prime ($'$) denotes the derivative with respect to η. The corresponding boundary conditions are

$$W = \Theta = 0 \text{ at } \eta = 0 \text{ and } W = \Theta' = 0 \quad \text{at } \eta = 1$$

The axial pressure gradient can be determined by the requirement of global mass conservation:

$$\int_0^1 (\eta + C) W d\eta = 0$$

2.2 Linear Stability Analysis

The normal mode analysis [16] is employed to investigate the stability of the above considered basic flow. The dependent field variables are decomposed into a basic state variables and an infinitesimal disturbance. The velocity field, temperature and pressure are written as:

$$(u, v, w, \theta, p) = \left(\tilde{u}, \tilde{v}, W(\eta) + \tilde{w}, \Theta(\eta) + \widetilde{\theta}, P(z) + \tilde{p}\right)$$

These infinitesimal disturbances of corresponding field variables are split into the following normal mode form as:

$$\left(\tilde{\boldsymbol{u}}, \tilde{\theta}, \tilde{p}\right) = \left(\hat{\boldsymbol{u}}(\eta), \hat{\theta}(\eta), \hat{p}(\eta)\right) e^{(i[\alpha(z-ct)+n\psi])} \tag{9}$$

where $\boldsymbol{u} = (u, v, w)$, α, $c = \widehat{c_r} + i\widehat{c_i}$, and n are the velocity field, axial wavenumber, complex disturbance wave speed, and azimuthal wavenumber, respectively. Upon substitution of equations above decomposition into the non-dimensional governing equations and neglecting the nonlinear terms, the linearized perturbation equations are given as follows:

$$\hat{u}\prime + \frac{\hat{u}}{\eta + C} + \frac{in\hat{v}}{\eta + C} + i\alpha\hat{w} = 0,$$

$$Gr\left[i\alpha(W - c)\hat{u} + \hat{p}\prime\right] - \hat{u}'' - \frac{\hat{u}\prime}{\eta + C} + \frac{\left(1 + n^2\right)\hat{u}}{(\eta + C)^2} + \left(\alpha^2 + \frac{1}{Da}\right)\hat{u} + 2in\frac{\hat{v}}{(\eta + C)^2} = 0,$$

$$iGr\left[\alpha(W - c)\hat{v} + \frac{n\hat{p}}{\eta + C}\right] - \hat{v}'' - \frac{\hat{v}\prime}{\eta + C} + \frac{\left(1 + n^2\right)\hat{v}}{(\eta + C)^2} + \left(\alpha^2 + \frac{1}{Da}\right)\hat{v} - 2in\frac{\hat{u}}{(\eta + C)^2} = 0,$$

$$Gr\left[i\alpha\left\{(W - c)\hat{w} + \hat{p}\right\} + W'\hat{u}\right] - \hat{w}'' - \frac{\hat{w}\prime}{\eta + C} + \frac{n^2\hat{w}}{(\eta + C)^2} + \left(\alpha^2 + \frac{1}{Da}\right)\hat{w} + \hat{\theta} = 0,$$

$$-GrPr\left[i\alpha(W - c)\hat{\theta} - \Theta'^{\hat{u}}\right] + \hat{\theta}'' + \frac{\hat{\theta}\prime}{\eta + C} - \frac{n^2\hat{\theta}}{(\eta + C)^2} - \alpha^2\hat{\theta} = 0.$$

Here, prime ($'$) denotes the first order derivative of a field variable with respect to η. The boundary conditions required to solved of the perturbation equations are

$$\hat{u}(0) = \hat{v}(0) = \hat{w}(0) = \hat{\theta}(0) = 0 \quad \text{and}$$
$$\hat{u}(1) = \hat{v}(1) = \hat{w}(1) = \hat{\theta}\prime(1) = 0.$$

Table 1 Validation of present results with the published results of Rogers and Yao [12] for different values of Pr, C and n

(Pr, C, n)	Published results [12]	Present results
	(Gr_c, α_c, c_r)	(Gr_c, α_c, c_r)
(0.01, 0.6, 1)	$(13900, 2.5, 0.19 \times 10^{-2})$	$(13913.2, 2.5, 0.20 \times 10^{-2})$
(0.01, 10, 0)	$(15140, 2.73, 0.42 \times 10^{-2})$	$(15135.4, 2.73, 0.42 \times 10^{-2})$
(10, 10, 0)	$(5526, 1.58, 0.43 \times 10^{-2})$	$(5520.6, 1.58, 0.43 \times 10^{-2})$
(10, 100, 1) and (10, 100, 0)	(6100, 1.52,)	(6086.6, 1.52,)

The basic flow equations as well as linear disturbance equations are solved by using spectral collocation method. The Chebyshev polynomials are used to approximate the dependent field variables. The domain [0, 1] is transformed to the canonical domain of Chebyshev polynomials by using transformation, $\xi = 2\eta - 1$. The highest order of Chebyshev polynomial used in the approximation of velocity, temperature and pressure fields is 80. The procedure of solving the linear disturbance equations and finding the critical value of controlling parameters is well explained in ref. [17]. To validate the presented numerical results, we have computed the critical value of Grashof number, the critical value of axial wavenumber, and critical wave speed for different values of C and Pr to the special case of purely viscous media flow [12] by setting $Da = 10^{12}$. Table 1 provides good support for the present results.

3 Results and Discussion

The parameters in this problem are Gr, Pr, C and Da. For a fixed Pr, C and Da, the flow becomes unstable as Gr increases and a complete linear instability map is obtained by considering the effect of Pr, C and Da on Grashof number. In this article, the impact of Pr on Gr is examined for two values (0.1 and 10) of C, three values (10^{-1}, 10^{-2} and 10^{-3}) of Da and a wide range $[10^{-3}, 10^{2}]$ of Prandtl number. The current choice of Pr provides a complete picture of the instabilities present in the considered physical scenario. It is worthwhile to note that the ideal gases will have Prandtl numbers greater than 0.4, which is known from kinetic theory, while most common liquids have Prandtl numbers greater than 1. The exceptions are liquid metals, whose Prandtl numbers are less than 0.1. Consequently, no common fluids will have Prandtl numbers in the intermediate range. However, data are presented for a continuous range of Prandtl number to demonstrate the results of the instability calculations.

It is crucial to understand how controlling parameters C and Da affect the point of inflection's appearance since the point of inflection on the basic flow velocity profile acts as a possibility for the flow instability [18]. In this connection, we have shown the basic flow velocity (W) for different value of both curvature parameter and Rayleigh number, as shown in Fig. 1a. The corresponding basic flow temperature (Θ) profile

displayed in Fig. 1b. The velocity profile for $C = 10$ is almost symmetric about $\eta = 0.5$, while the profile for $C = 0.1$ is asymmetric. This is because $C = 10$ corresponds to an annulus with a narrow gap, approaching a two-dimensional slot, while $C = 0.1$ represents an annulus with a much more pronounced curvature effect. Both of these velocity profiles contain inflection points, which suggests a potential for inviscid instability. Moreover, it can be seen from the velocity profiles that on changing the value of curvature parameter from 0.1 to 10, the point of inflection shifts from the inner cylinder to the center of the annular domain. However, on decreasing the media permeability, the same shifts from the center to the inner cylinder. On increasing the value of C, the maximum magnitude of the velocity decreases representing the stabilizing nature of C. The media permeability played just a reverse role in the stability of the flow. The temperature profile does not influence by the media permeability for a fixed gap between cylinders, whereas a significant impact of C is visible in Fig. 1b.

The linear instability boundary for the considered set of parameters is shown in Fig. 2a and b. Figure 2a represents the graph of critical value of Gr (i.e., Gr_c) as a function of Pr for $C = 0.1$ and Fig. 2b represents the same for $C = 10$. The solid line in each figure demonstrates the Gr_c-profile for two-dimensional axisymmetric disturbance, whereas the dashed line demonstrate the Gr_c-profile for three-dimensional non-axisymmetric disturbance. It can be seen that the least stable disturbance may be axisymmetric or non-axisymmetric depending on the value of C. For smaller value of C, the least stable disturbance are always three-dimensional, i.e., non-axisymmetric (see Fig. 2a). However, for larger value of C, the least stable disturbance are always

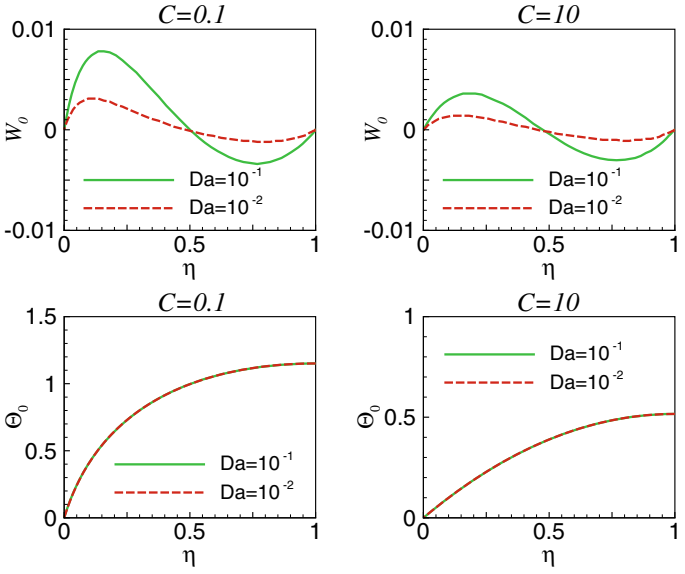

Fig. 1 Base flow velocity and temperature profile for different values of C and Da. The green solid line and red dashed line correspond to $Da = 10^{-1}$ and $Da = 10^{-2}$

two-dimensional, i.e., axisymmetric (see Fig. 2b). The solid and dashed lines in the same figure appear to overlap, but after closely examining the data, we found that the solid line is always lower than the dashed line, signifying that the axisymmetric disturbance is most unstable. On decreasing the media permeability in terms of *Da*, the critical value of the Grashof number increases for both values of *C*. Further, an increase in the curvature parameter results in an increase in the critical value of Grashof number, demonstrating the stabilizing nature of *C*. In general, it can be seen from both figures that on increasing the value of *Pr*, the critical value of *Gr* decreases rapidly up to a threshold value of Prandtl number, and above that threshold value of Prandtl number the change in Gr_c is smooth and gradual. To get a greater understanding of the variation of instability boundary, we have taken the help of kinetic energy budget [17]. To derive the balance of kinetic energy, the disturbed velocity field is multiplied on both sides of the disturbed momentum equations (before substituting the normal mode form of the disturbance), which are then integrated over the volume: $[0,\ 1] \times [0,\ 2\pi/\alpha] \times [0,\ 2\pi/n]$ of the disturbance cell. Thus, the rate of change of kinetic energy balance is given as

$$\frac{Gr}{\varepsilon}\frac{\partial}{\partial t}\frac{1}{2}\left(\tilde{u}^2+\tilde{v}^2+\tilde{w}^2\right) = -\tilde{w}\tilde{\theta} - \frac{1}{Da}\left(\tilde{u}^2+\tilde{v}^2+\tilde{w}^2\right) - (\nabla\tilde{u})^2 + (\nabla\tilde{v})^2 + (\nabla\tilde{w})^2 = E_b + E_D + E_d$$

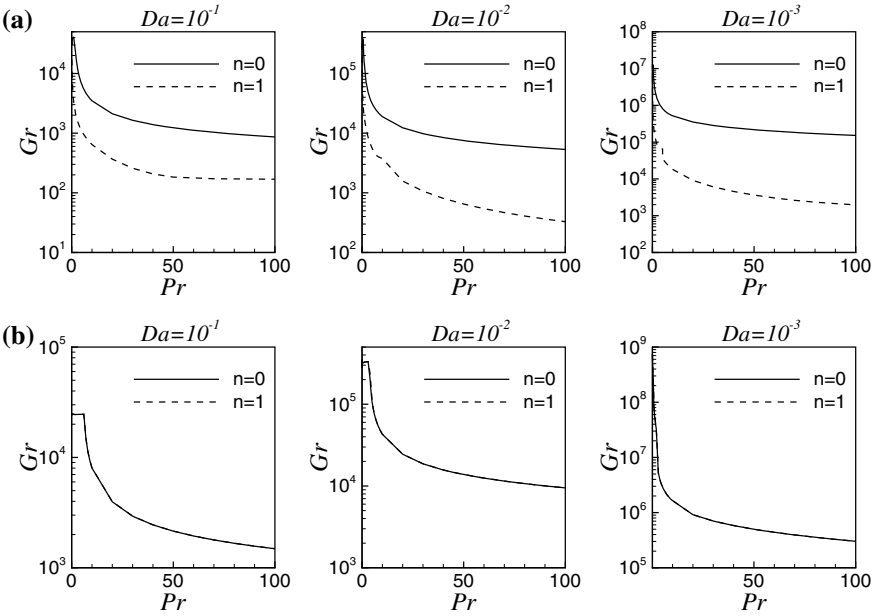

Fig. 2 Linear instability boundary as a function of Prandtl number in (*Pr*, *Gr*)- plane for **a** $C = 0.1$ and **b** $C = 10$

In the above equation, the symbol ⟨ ⟩ indicates the integration over the volume of a disturbance cell. In Eq. (20), the integrands in the above equation can be calculated by using the eigenvectors from the linear stability theory. The left-hand side of the Eq. (20) is zero at the critical values of controlling parameter because the disturbances neither grow nor decay along neutral-stability boundary. On the right side of the Eq. (20), the three terms E_D, E_d, and E_b stand for the dissipation of kinetic energy due to work done by surface drag, the dissipation of kinetic energy due to viscous effects, and the production of kinetic energy through work done by the fluctuating body force, respectively. Overall, KE balance Eq. (20) depicts a balance between the dissipation of disturbance kinetic energy caused by viscous force and surface dragand the production of disturbance kinetic energy caused by the buoyant mechanism. Figure 2 clearly indicates that at larger values of *Pr,* the dominant instability is insensitive to changes in *Pr* for both values of *C*. Moreover, the critical value of axial wavenumber shows an asymptotic nature (figure not shown). On the other hand, at smaller values of *Pr*, instability appears which is strongly dependent on *Pr*, with *Gr*, decreasing with increasing *Pr*. Moreover, in the case of purely viscous media [12], at larger values of the Prandtl number, the flow instability is strongly dependent on *Pr*, with *Gr*, decreasing with increasing *Pr,* whereas at small values of *Pr,* the dominant instability is insensitive to changes in *Pr*. In the present case, at a large value of *Pr*, the buoyant production is balanced by the dissipation of disturbance kinetic energy, which is due to the effect of viscosity as well as surface drag. Therefore, for all considered values of *Da* and *C*, the type of instability is thermal-buoyant. In this instance, for a high value of *Pr*, the buoyant production is counterbalanced by the dissipation of disturbance kinetic energy, which is caused by the impact of viscosity as well as surface drag. In all cases when *Da* and *C* are taken into consideration, the kind of instability is thermal-buoyant. Additionally, the buoyant, viscous and surface drag disturbance forces acting on the flow through the porous material cause the point of inflection in the basic velocity profile to exist or not appear.

4 Conclusions

The present work considered the linear stability analysis of stably stratified non-isothermal parallel flow through a vertically oriented annular domain filled with porous material. The point of inflection in the considered stable laminar flow results in flow instability. The flow is stabilized by the curvature parameter, which is described in terms of the space between the coaxial circular cylinders. The media permeability has a destabilizing impact on the flow. The fluid with a relatively low Prandtl number is linearly most stable against non-axisymmetric disturbance whereas the fluid with relatively high *Pr* is linearly most stable against axisymmetric disturbance. When the Prandtl number is comparatively bigger, the kinetic energy budget shows that the dominating instability predominantly derives its energy through buoyant production.

To acquire a comprehensive view of the transition to turbulence, the influence of the Prandtl number on the type of bifurcation and secondary flow pattern may also

be studied via nonlinear stability analysis of the same problem. These analyses are left for our future study.

Acknowledgements The author A.K. is grateful to *IIT Delhi*, India for providing the *institute postdoctoral research fellowship* to carry the present work.

References

1. Venugopal G, Balaji C, Venkateshan SP (2010) Experimental study of mixed convection heat transfer in a vertical duct filled with metallic porous structures. Int J Therm Sci 49:340–348
2. Nield DA, Bejan A (2013) Convection in porous media. Springer, New York
3. Orr FM (2010) Onshore geologic storage of co_2. Science 325:1656–1658
4. Lorente S, Petit M, Javelas R (1998) The effects of temperature conditions on the thermal resistance of walls made of different shapes vertical hollow bricks. Energy Build 28:237–240
5. Shankar BM, Kumar J, Shivakumara IS (2017) Stability of natural convection in a vertical layer of brinkman porous medium. Acta Mech 228:1–19
6. Sharma AK, Bera P (2018) Linear stability of mixed convection in a differentially heated vertical channel filled with high permeable porous-medium. Intl J Therm Sci 134:622–638
7. Choueiri GH, Tavoularis S (2015) Experimental investigation of flow development and gap vortex street in an eccentric annular channel. Part 2. Effects of inlet conditions, diameter ratio, eccentricity and Reynolds number. J Fluid Mech 768:294–315
8. Orihuela MP, Anuar FS, Abdi IA, Odabaee M, Hooman K (2018) Thermohydraulics of a metal foamfilled annulus, Intl. J Heat Mass Transfer 117:95–106
9. Khan A, Bera P (2022) Weakly nonlinear analysis of non- isothermal parallel flow in a vertical annulus filled with porous medium. Available at SSRN: https://ssrn.com/abstract=4210152 or https://doi.org/10.2139/ssrn.4210152
10. Bringedal C, Berre I, Nordbotten JM, Rees DAS (2011) Linear and nonlinear convection in porous media between coaxial cylinders. Phys Fluids 23:094109–094111
11. Barletta A, Celli M, Rees DAS (2020) Buoyant flow and instability in a vertical cylindrical porous slab with permeable boundaries. Intl J. Heat Mass Transf 157:119956
12. Rogers BB, Yao LS (1993) Natural convection in a heated annulus. Intl J Heat Mass Transfer 36:35–47
13. Elder JW (1965) Turbulent free convection in a vertical slot. Intl J Fluid Mech 23:99–111
14. Choi G, Korpela SA (1980) Stability of the conduction regime of natural convection in a tall vertical annulus. J Fluid Mech 99:725–738
15. Whitaker S (1996) The forchheimer equation: a theoretical development. Transp Porous Media 25:27–61
16. Drazin PG, Reid WH (2004) Hydrodynamic stability. Cambridge University Press
17. Khan A, Bera P (2020) Linear instability of concentric annular flow: effect of Prandtl number and gap between cylinders. Int J Heat Mass Transf 152:119530
18. Khan A, Bera P, Khandelwal MK (2019) Bifurcation and instability of mixed convection in a vertical annulus: dependence on curvature parameter. Phys Fluids 31:104105-1–104120